GEOPHYSICAL RESEARCH LETTERS, VOL. 25, NO. 3, PAGES 309-312, FEBRUARY 1, 1998

Depolarization of lidar returns by small ice crystals: An application to contrails

Michael I. Mishchenko
NASA Goddard Institute for Space Studies, New York, New York

Kenneth Sassen
The University of Utah, Salt Lake City, Utah

Abstract. Measurements of the lidar linear depolarization ratio δ can be a powerful remote sensing technique for characterizing the microphysics of contrail particles. Since young contrails often consist of relatively small ice crystals, the quantitative interpretation of lidar measurements requires accurate theoretical computations of δ for polydisperse, randomly oriented nonspherical particles with size parameters ranging from zero to at least several tens, thus ruling out most of the currently available numerical techniques. In this paper we use the recently improved *T*-matrix method and compute δ for polydispersions of randomly oriented ice spheroids, circular cylinders, and Chebyshev particles with sizes typical of young contrails. We show that ice crystals with effective radii as small as several tenths of a micron can already produce δ exceeding 0.5 at visible wavelengths. This may explain the frequent occurrence of large δ values for very young contrails. We also show that observed increases of δ with the contrail's age can be explained either by a rapid increase of the particle size parameter from essentially zero to about 5 or by assuming that the contrail particles originate as perfect spheres and then acquire a certain degree of asphericity.

1. Introduction

Because of intensifying air traffic, there has been increasing interest in the potential impact of aircraft condensation trails (contrails) on climate through a direct radiative forcing. The estimation of the climatic effect of contrails requires knowledge of their radiative properties, which can be substantially different from those of ambient cirrus clouds [*Sassen*, 1997; *Spinhirne et al.*, 1997]. The latter, in turn, necessitates the determination of the size and shape distribution of contrail particles and their time evolution using in situ and/or remote sensing techniques.

Polarization lidar is a powerful remote sensing method for characterizing the microphysics of ice cloud particles because it helps to infer the shape of hydrometeors [*Sassen*, 1991; *Eberhard*, 1992; *Stefanutti et al.*, 1995; *Aydin and Tang*, 1997]. Recent lidar measurements of contrails at a visible wavelength of λ = 0.532 μm [*Freudenthaler et al.*, 1996] have shown that the linear depolarization ratio can be large even for very young contrail particles, can change significantly with the age of the contrails, and depends on the ambient temperature. The quantitative interpretation of these measurements requires accurate depolarization calculations for polydisperse, randomly oriented nonspherical particles with size parameters ranging from zero to at least several tens, thus making it difficult to apply techniques such as the discrete dipole approximation, finite difference time domain method, and geometric optics (GO) approximation. Therefore, in this paper we analyze the lidar observations of contrails using a much more efficient *T*-matrix method [*Mishchenko et al.*, 1996a]. Recent improvements have extended this technique to significantly larger size parameters, making it more suitable for computations of young contrails.

Paper number 97GL03764.
0094-8534/98/97GL-03764$05.00

2. *T*-matrix Computations

In most cases contrail particles appear to be too small to become partially oriented by the aerodynamical force resulting from their finite falling velocity [*Sassen*, 1980]. We will, therefore, assume that contrail crystals are fully randomly oriented in 3-D space. Assuming also a reasonable symmetry and/or diversity of ice particle shapes and using the standard Stokes $\{I,Q,U,V\}$ representation of polarization, we have that the scattering matrix in the exact backscattering direction is diagonal and given by $\mathbf{F}(180°) = \mathrm{diag}[F_{11}(180°), F_{22}(180°), F_{33}(180°), F_{44}(180°)]$ [*Mishchenko and Hovenier*, 1995]. Let us choose a fixed plane through the direction of the transmitted lidar beam and use it as a reference plane for defining the Stokes parameters. If the transmitted beam is 100% linearly polarized parallel to this plane, its Stokes vector is proportional to {1, 1, 0, 0}. The linear depolarization ratio δ is defined as the ratio of the flux of the cross-polarized component of the backscattered light relative to that of the co-polarized component. Given the structure of the Stokes backscattering matrix, we have $\delta = [F_{11}(180°) - F_{22}(180°)] / [F_{11}(180°) + F_{22}(180°)]$. For spherical particles $F_{11}(180°) \equiv F_{22}(180°)$, thus causing a zero depolarization ratio. Therefore, any deviation of δ from zero can be a direct indication of the presence of nonspherical particles provided that the optical thickness of a contrail is relatively small and does not cause significant depolarization due to multiple scattering [*Sassen*, 1991].

It is well known that the optical cross sections and the scattering matrix elements for monodisperse particles strongly oscillate with varying size parameter and/or scattering angle [*Hansen and Travis*, 1974; *Mishchenko et al.*, 1996a]. These oscillations are caused by interference effects and make it very difficult to interpret calculations for particles of a single size. In practice, however, the interference structure is almost never observed due to the smoothing effect of the distribution of natural particles over size. This suggests that a meaningful analysis of the lidar depolarization observations of contrails must be based on calculations for realistic particle polydispersions rather than on monodisperse computations. Other factors that must be taken into consideration are that accurate scattering calculations are especially demanding at the exact backscattering direction [*Bohren and Singham*, 1991], that computations of the scattering matrix elements are often much more difficult than equally accurate computations of the total optical cross sections [*Okamoto et al.*, 1995; *Wielaard et* *al.*, 1997], and that the volume- or surface-equivalent sphere size parameter for contrail particles can range from almost zero to at least several tens [*Sassen*, 1997]. These complex factors rule out essentially all existing numerical techniques except the *T*-matrix method. A shortcoming of the current version of the *T*-matrix code described by *Mishchenko et al.* [1996a,b] is that it is applicable only to rotationally symmetric particles with moderate aspect ratios. However, small contrail particles rarely form aggregates and usually have relatively simple geometry [*Sassen*, 1997]. Furthermore, *T*-matrix calculations can still be performed for a great variety of shapes such as prolate and oblate spheroids with different aspect ratios, circular cylinders with varying length-to-diameter ratios, and so-called Chebyshev particles [*Wiscombe and Mugnai*, 1986]. In particular, we expect that spheroids and Chebyshev particles can reasonably represent ice crystals with smooth surfaces, while cylinders may represent hexagonal columns and plates.

As for the particle size distribution, *Hansen and Travis* [1974] have demonstrated that most plausible size distributions can be well represented by just two parameters, the effective radius r_{eff} and effective variance v_{eff}. Specifically, different size distributions which have the same r_{eff} and v_{eff} can be expected to have similar scattering properties. We have adopted for this study a simple power law distribution given by $n(r) = C$ for $r \leq r_1$, $n(r) = C(r_1/r)^3$ for $r_1 \leq r \leq r_2$, and $n(r) = 0$ for $r > r_2$, where C is a normalization constant, and r is the surface-equivalent-sphere radius. The parameters r_1 and r_2 are chosen such that the effective variance is fixed at 0.1, corresponding to a moderately wide distribution. An important advantage of the power law distribution is that for the same v_{eff}, it has a (much) smaller value of the maximum radius r_2 than optically equivalent gamma and log normal distributions, thus significantly accelerating light scattering computations.

Figure 1 shows δ versus the effective size parameter $x_{\text{eff}} = 2\pi r_{\text{eff}}/\lambda$ for a representative selection of ice particle shapes. The refractive index of $1.308 + 1.328 \times 10^{-6}i$ is typical of water ice at visible wavelengths [*Warren*, 1984]. For spheroids, ε is the ratio of the largest to the smallest semi-axes. Shapes of prolate and oblate cylinders are specified by length-to-diameter and diameter-to-length ratios, respectively. The shape of a second-order Chebyshev particle in a spherical coordinate system is described by the equation $r(\vartheta, \varphi) = r_0 [1 + \varepsilon \cos 2\vartheta]$, where ε is a deformation parameter specifying the maximum deviation of the particle shape from that of a sphere with radius r_0. Three-dimensional drawings of Chebyshev particles can be found in *Mannoni et al.* [1996]. The calculations took 3 months of CPU time on an IBM RISC model 39H workstation and include data for 60,000 particles with monodisperse equivalent-sphere size parameters up to 50.

Some lidars measure the circular, δ_C, rather than the linear depolarization ratio. δ_C can be easily computed using data given in Figure 1 and the general relationship $\delta_C = 2\delta/(1-\delta)$ [*Mishchenko and Hovenier*, 1995].

3. Discussion and Conclusions

Figure 1 shows that an interesting and important feature of the depolarization curves for essentially all shapes studied is a rapid increase of δ with increasing x_{eff} from 0 to about 5. Furthermore, maximal δ values for most shapes are observed at effective size parameters close to and sometimes smaller than 10. Since geometric optics concepts of rays, reflections, and refractions are inapplicable to wavelength- and sub-wavelength-sized particles, our computations demonstrate that multiple internal reflections in very large particles, as discussed by *Liou and Lahore* [1974], are not the only mechanism of producing depolarization and not necessarily the mechanism producing maximal δ values. For example, the peak δ value for polydisperse prolate spheroids with $\varepsilon = 1.2$ is close to 0.7 and is reached at x_{eff} as small as 12.5. Furthermore, monodisperse particles of the same shape produce depolarization ratios exceeding 0.8 [cf. *Mishchenko and Hovenier*, 1995]. Also, GO predicts size-parameter-independent depolarization ratios for nonabsorbing particles, whereas exact *T*-matrix computations for monodisperse scatterers show a strong interference structure [*Mishchenko and Hovenier*, 1995]. It thus appears that resonance effects in small nonspherical particles can be an efficient alternative mechanism of producing strong depolarization.

The computations show no strong relationship between δ and the degree of particle asphericity (i.e., ratio of the largest to the smallest particle dimensions). Even spheroids with ε as small as 1.05 (2.5% deviation from the perfect spherical shape) and Chebyshev particles with $|\varepsilon|$ as small as 0.02 already produce strong depolarization. The largest δ values are produced by prolate spheroids with aspect ratio as small as 1.2 and Chebyshev particles with ε as small as $0.08-0.10$ ($8-10$% deviation from a sphere). Furthermore, δ for spheroids and, especially, cylinders seems to saturate with increasing aspect ratio. Also of interest is that smooth scatterers (spheroids and Chebyshev particles) produce depolarization ratios comparable to and even exceeding those for sharp-edged cylinders.

The most important conclusion following from Figure 1 is that polydisperse, randomly oriented, wavelength-sized nonspherical ice crystals can indeed produce strong depolarization typical of natural cirrus particles. It has often been observed that young contrails can consist of much smaller particles than ambient cirrus [e.g., *Sassen*, 1997]. Therefore, it has been unclear whether such small particles, for which the GO mechanism of multiple internal reflections does not apply, can reproduce the observed large δ values [*Freudenthaler et al.*, 1996; *Sassen and Hsueh*, 1998]. Our extensive computations demonstrate that ice crystals with effective radii greater than several tenths of a micron can already produce depolarization ratios exceeding 0.5 at visible wavelengths. This appears to explain the frequent occurrence of large δ values for contrails with age less than 20 s [*Freudenthaler et al.*, 1996] and indicates that the number density of small contrail particles can be large enough to produce a measurable signal. The only particles that cannot produce the highest observed values $\delta \approx 0.4-0.55$ are prolate ice cylinders.

Our computations show that the initial increase in lidar linear depolarization with contrail age observed by *Freudenthaler et al.* [1996] at temperatures below $-55°$C can be explained either by a rapid increase in particle size parameter from near-zero to about 5, or by assuming that the contrail particles originated as spheres and then acquired a certain degree of asphericity. In terms of the 0.532 μm lidar wavelength used in recent studies [*Freudenthaler et al.*, 1996; *Sassen*, 1997], contrail particle sizes of <1 μm diameter would be needed to generate the unusually low (<0.1) δ values.

It should be acknowledged that the interpretation of lidar depolarization is further complicated in this case by uncertainties in the compositions of jet engine exhaust-contaminated contrail particles, including soot-containing inhomogeneous particles, highly supercooled sulfuric acid haze droplets and the contaminated ice crystals nucleated from them, and even more exotic mixed-composition crystals involving water ice and frozen nitric acid (NAT) particles [*Sassen*, 1997]. Nonetheless, our interpretation of recent lidar data in terms of the current theory leads us to conclude that the low depolarization ratios in cold, young contrails can be most confidently explained by extremely small (<1 μm diameter) contrail ice crystals; the alternative explanation of almost

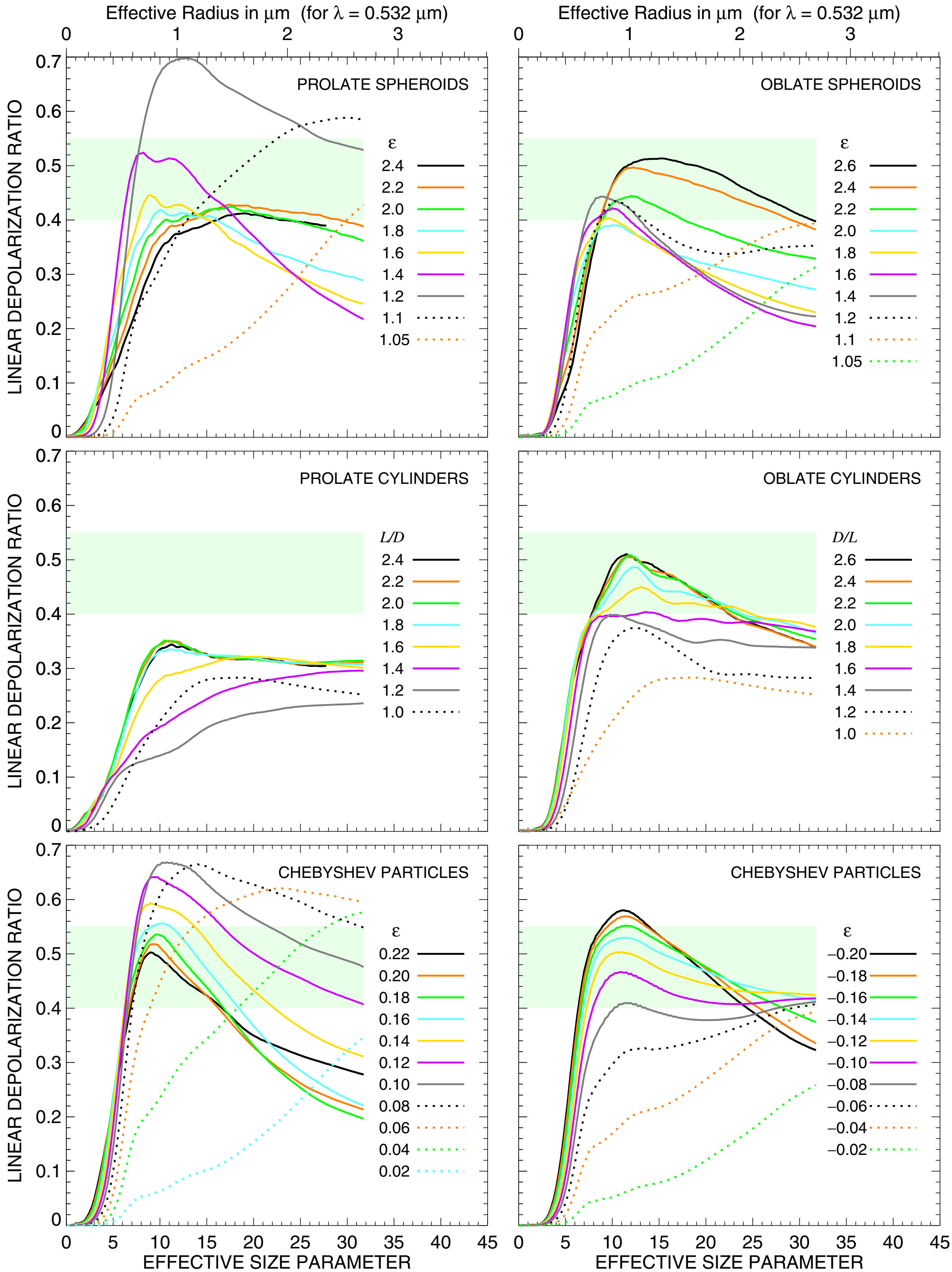

Figure 1. Linear depolarization ratio versus effective size parameter for polydisperse, randomly oriented ice particles of different shapes. The light green area shows the highest range of depolarization ratios observed for contrail particles by *Freudenthaler et al.* [1996]. The upper x axes convert x_{eff} to r_{eff} assuming $\lambda = 0.532$ μm.

perfectly-spherical shapes (deviating from a true sphere by less than 2%) is unlikely according to current knowledge of particle growth in the upper troposphere. We note that additional polarization lidar studies of a young ($\sim 0.5-8$ min old) contrail recently reported by *Sassen and Hsueh* [1998] show a decrease in δ from 0.68 to 0.38, which conforms well with the effects of a gradual increase in particle size with time according to Fig. 1. Moreover, contrails on the order of 1 h old yielded a large range ($\sim 0.3-0.7$) in δ values, indicating that more mature ice crystal shapes in persisting contrails can be quite varied.

The apparent temperature dependence noted by *Freudenthaler et al.* [1996] in the occurrence of low contrail δ values can probably be explained by the overwhelming temperature dependence in both the rates of homogeneous nucleation of solution droplets and ice crystal growth. This combination of effects would likely lead to relatively more numerous and smaller ice crystals as environmental temperatures decrease. The model simulations of *Gierens* [1996] show the effect of ice crystal growth rate on contrail content, even though ice crystal nucleation as a function of temperature was not explicitly treated.

Finally we note that in view of the apparent strong depolarization dependence on the size of ice particles typical of young contrails, dual-wavelength polarization systems like the Polarization Diversity Lidar employed by *Sassen and Hsueh* [1998] should be very useful for studying the evolution in contrail particle mean size.

Acknowledgments. We thank two anonymous reviewers for useful comments, B. Cairns for helpful discussions, and N. T. Zakharova for assistance with graphics. This research was funded by the NASA Atmospheric Effects of Aviation Project, NSF grant ATM-94134337, and NRL grant N00014-96-1-G020.

References

Aydin, K., and C. Tang, Millimeter wave radar scattering from model ice crystal distributions, *IEEE Trans. Geosci. Rem. Sens.*, *35*, 140-146, 1997.

Bohren, C. F., and S. B. Singham, Backscattering by nonspherical particles: A review of methods and suggested new approaches, *J. Geophys. Res.*, *96*, 5269-5277, 1991.

Eberhard, W. L., Ice-cloud depolarization of backscatter for CO_2 and other infrared lidars, *Appl. Opt.*, *31*, 6485-6490, 1992.

Freudenthaler, V., F. Homburg, and H. Jäger, Optical parameters of contrails from lidar measurements: lidar depolarization, *Geophys. Res. Lett.*, *23*, 3715-3718, 1996.

Gierens, K. M., Numerical simulations of persistent contrails, *J. Atmos. Sci.*, *53*, 3333-3348, 1996.

Hansen, J. E., and L. D. Travis, Light scattering in planetary atmospheres, *Space Sci. Rev.*, *16*, 527-610, 1974.

Liou, K.-N., and H. Lahore, Laser sensing of cloud composition: a backscatter depolarization technique, *J. Appl. Meteorol.*, *13*, 257-263, 1974.

Mannoni, A., C. Flesia, P. Bruscaglioni, and A. Ismaelli, Multiple scattering from Chebyshev particles: Monte Carlo simulations for lidar geometry, *Appl. Opt.*, *35*, 7151-7164, 1996.

Mishchenko, M. I., and J. W. Hovenier, Depolarization of light backscattered by randomly oriented nonspherical particles, *Opt. Lett.*, *20*, 1356-1358, 1995.

Mishchenko, M. I., L. D. Travis, and D. W. Mackowski, *T*-matrix computations of light scattering by nonspherical particles: A review, *J. Quant. Spectrosc. Radiat. Transfer*, *55*, 535-575, 1996a.

Mishchenko, M. I., L. D. Travis, and A. Macke, Scattering of light by polydisperse, randomly oriented, finite circular cylinders, *Appl. Opt.*, *35*, 4927-4940, 1996b.

Okamoto, H., A. Macke, M. Quante, and E. Raschke, Modeling of backscattering by nonspherical ice particles for the interpretation of cloud radar signals at 94 GHz. An error analysis, *Contr. Atmos. Phys.*, *68*, 319-334, 1995.

Sassen, K., Remote sensing of planar ice crystal fall attitudes, *J. Meteorol. Soc. Japan*, *58*, 422-429, 1980.

Sassen, K., The polarization lidar technique for cloud research: a review and current assessment, *Bull. Am. Meteorol. Soc.*, *72*, 1848-1866, 1991.

Sassen, K., Contrail-cirrus and their potential for regional climate change, *Bull. Am. Meteorol. Soc.*, *78*, 1885-1903, 1997.

Sassen, K., and C.-Y. Hsueh, Contrail properties derived from high-resolution polarization lidar studies during SUCCESS, *Geophys. Res. Lett.*, in press, 1998.

Spinhirne, J. D., D. Duda, and W. D. Hart, Contrail microphysics and radiative properties from aircraft remote sensing in SUCCESS, *EOS Trans. AGU*, *78*, Spr. Meet. Suppl., S96, 1997.

Stefanutti, L., M. Morandi, M. Del Guasta, S. Godin, and C. David, Unusual PSCs observed by LIDAR in Antarctica, *Geophys. Res. Lett.*, *22*, 2377-2380, 1995.

Warren, S. G., Optical constants of ice from the ultraviolet to the microwave, *Appl. Opt.*, *23*, 1206-1225, 1984.

Wielaard, D. J., M. I. Mishchenko, A. Macke, and B. E. Carlson, Improved *T*-matrix computations for large, nonabsorbing and weakly absorbing nonspherical particles and comparison with geometric optics approximation, *Appl. Opt.*, *36*, 4305-4313, 1997.

Wiscombe, W. J., and A. Mugnai, Single scattering from nonspherical Chebyshev particles: A compendium of calculations, *NASA Ref. Publ.*, *1157*, 1986.

M. I. Mishchenko, NASA GISS, 2880 Broadway, New York, New York 10025. (e-mail: crmim@giss.nasa. gov)

K. Sassen, Department of Meteorology, The University of Utah, 819 Wm. C. Browning Bldg., Salt Lake City, Utah 84112. (e-mail: ksassen@atmos.met.utah.edu)

(Received August 22, 1997; revised December 1, 1997; accepted December 19, 1997)